NASA TECHNICAL NOTE

NASA TN D-2466

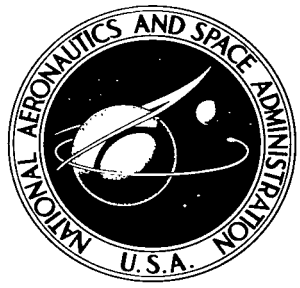

NASA TN D-2466

LOAN COPY: RETURN
AFWL (WLIL-2)
KIRTLAND AFB, N ME

TECH LIBRARY KAFB, NM
0079553

COMPARISON OF GROUND TESTS AND ORBITAL LAUNCH RESULTS FOR THE EXPLORER IX AND EXPLORER XIX SATELLITES

by Charles V. Woerner and Claude W. Coffee, Jr.

Langley Research Center
Langley Station, Hampton, Va.

NATIONAL AERONAUTICS AND SPACE ADMINISTRATION • WASHINGTON, D. C. • SEPTEMBER 1964

TECH LIBRARY KAFB, NM
0079553

COMPARISON OF GROUND TESTS AND ORBITAL LAUNCH RESULTS FOR THE EXPLORER IX AND EXPLORER XIX SATELLITES

By Charles V. Woerner and Claude W. Coffee, Jr.

Langley Research Center
Langley Station, Hampton, Va.

NATIONAL AERONAUTICS AND SPACE ADMINISTRATION

For sale by the Office of Technical Services, Department of Commerce,
Washington, D.C. 20230 -- Price $0.75

COMPARISON OF GROUND TESTS AND ORBITAL LAUNCH RESULTS FOR THE EXPLORER IX AND EXPLORER XIX SATELLITES

By Charles V. Woerner and Claude W. Coffee, Jr.
Langley Research Center

SUMMARY

A study has been made of the flight-test results for the launch and orbiting of the 12-foot-diameter inflatable spheres, Explorer IX and Explorer XIX. The two flight tests have demonstrated that, in general, the in-flight operation of the ejection and inflation system was similar to that experienced during environmental tests and that a lightweight delicate structure can be erected in space after withstanding the severe conditions imposed by an orbiting spin-stabilized launch vehicle. The two flight tests have demonstrated that the longitudinally unrestrained folded sphere does not eject prematurely. The apparent magnitude, as reported by various Moonwatch teams, has shown very good agreement with theoretical calculations for an inflatable structure of this type.

INTRODUCTION

The present values of atmospheric density at satellite altitudes are inferred from the orbital decay rates of satellites of various sizes and shapes. Many of these satellites are not suited for this purpose since in most cases they are nonspherical and their frontal-area orientation is not known. These satellites are also inconveniently slow in obtaining data over a large range of altitudes because they have a large ratio of mass to area. Since orbital decay rates are more rapid for satellites having a small ratio of mass to area, a lightweight inflatable spherical satellite having a 12-foot diameter was designed and constructed by the Langley Research Center. (See ref. 1.) A 12-foot-diameter satellite was placed into orbit on February 16, 1961, by the Scout launching vehicle and designated Explorer IX (1961 Delta 1). The objectives of the Explorer IX satellite were: (1) to make air-density measurements at satellite altitudes between north and south latitudes of 38.91°; (2) to study the effects of solar perturbations on satellites of small ratio of mass to area; (3) to study the effects of a space environment on an inflatable structure.

A second 12-foot-diameter satellite was placed into a near polar orbit on December 19, 1963, by the Scout launching vehicle and was designated Explorer XIX. The major objectives of this air-density Explorer satellite are: (1) to extend the upper air-density measurements to the polar regions between

north and south latitudes of 78.62°; (2) to determine the latitude variations and temperature of the atmosphere; (3) to determine sources of atmospheric heating by comparing measurements with other satellites, such as the Explorer IX.

The purpose of this paper is to present the flight-test results for the launching of the Explorer IX satellite and to compare these flight-test results with ground tests in order to make an evaluation of the deployment system of the 12-foot-diameter satellite. Also, the results of the launch of the Explorer XIX satellite are presented.

DESCRIPTION OF PAYLOAD

A drawing showing the general arrangement of the fourth-stage rocket motor and its payload, the 12-foot-diameter inflatable sphere, in their launch configuration for Explorer IX is shown in figure 1. A photograph of the complete payload for Explorer IX is shown in figure 2. The weight breakdown of the assembled payload for Explorer IX is presented in table I. Photographs of the complete payload for Explorer XIX are shown in figure 3, and the weight breakdown of the assembled payload is presented in table II.

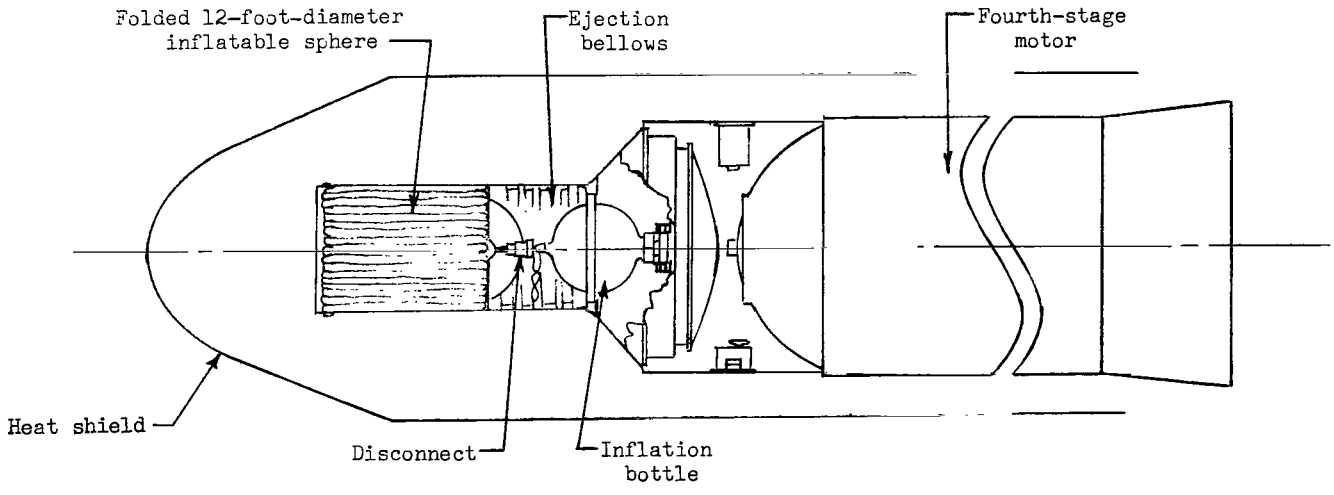

Figure 1.- General arrangement of fourth-stage rocket motor and Explorer IX payload, the 12-foot-diameter inflatable sphere.

Inflatable Satellite Package

Inflatable sphere.- A general description of the design, development, and fabrication of the inflatable spheres is given in reference 1. The spheres were constructed from a four-ply laminate consisting of alternate layers of 0.0005-inch-thick aluminum foil and 0.0005-inch-thick plastic film. The aluminum foil forms the outside surface of the sphere and the plastic film, the

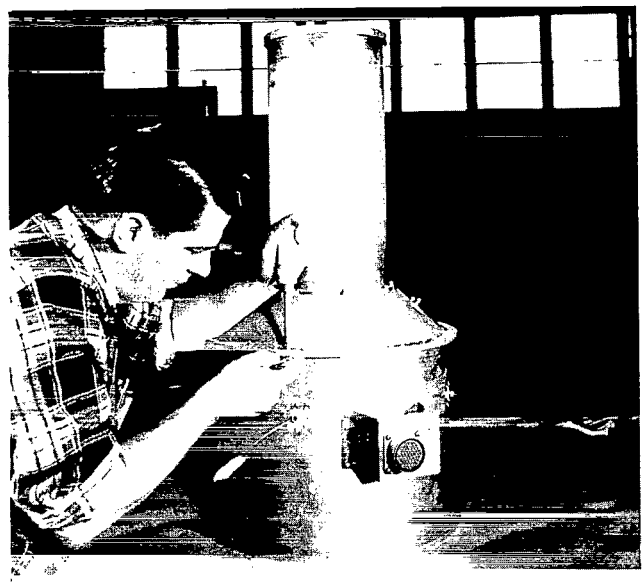

L-61-572

Figure 2.- Photograph of complete payload for launch of Explorer IX.

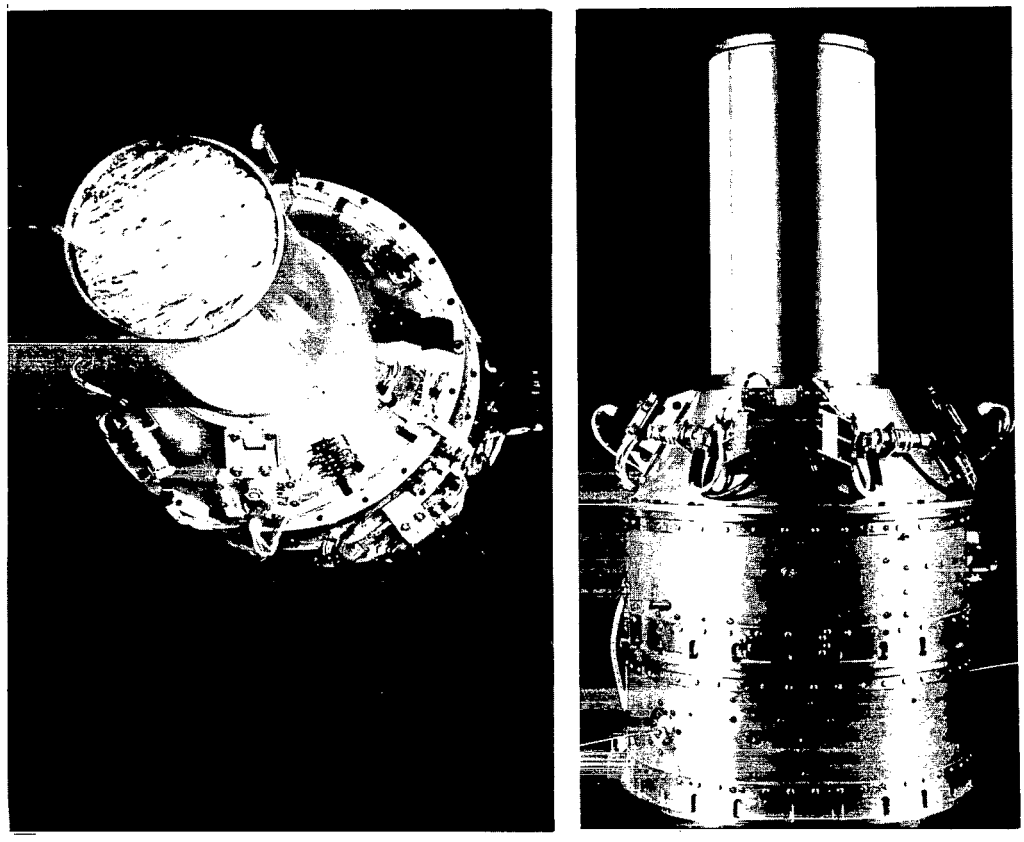

L-63-9620

L-63-9623

Figure 3.- Photographs of complete payload assembly for launch of Explorer XIX.

TABLE I.- WEIGHT BREAKDOWN OF EXPLORER IX PAYLOAD

	Weight, lb	
12-foot-diameter inflatable satellite:		
Sphere	12.470	
Solar-cell modules (4)	1.019	
Transmitter module	0.382	
Battery module	0.380	
Battery switch	0.014	
Thermal patch over transmitter and battery modules	0.040	
Plastic tape	0.102	
Copper cable	0.113	
Inflation-valve stem extension	0.100	
Total orbiting weight		14.62
Rubber spacers for packing folded sphere		1.14
Inflation bottle:		
Bottle, valve, squibs, and squib holder	4.20	
Inflation gas (nitrogen)	0.50	
Total		4.70
Activation batteries, pressure cell and switch, fairing switches, and electrical harness		7.00
Ejection bellows		2.02
Disconnect mechanism		0.54
Folded-sphere container and conical support section:		
Container	6.56	
Support section	4.52	
Total		11.08
Attachment collar and antennas		11.16
Payload telemeter and fourth-stage minitrack beacon		19.56
Miscellaneous:		
Container cover (foam-plastic sheet with metal strip)	0.26	
Screws, bolts, nuts, and so forth	0.70	
Total		0.96
Added weight:		
Static balance	2.21	
Dynamic balance	0.50	
Ballast	4.16	
Total		6.87
Total payload weight for launch		79.65

TABLE II.- WEIGHT BREAKDOWN OF EXPLORER XIX PAYLOAD

	Weight, lb	
12-foot-diameter inflatable satellite:		
Sphere	14.328	
Solar-cell modules (4)	2.186	
Transmitter module	0.512	
Battery-control module	0.486	
Battery switch	0.019	
White paint patches for transmitter and battery modules	0.016	
Wavelength antenna on equator	0.035	
Solar-cell collars (4)	0.034	
Inflation-valve stem extension	0.116	
Miscellaneous	0.056	
Total orbiting weight		17.79
Rubber spacers for packing folded sphere		1.53
Disconnect mechanism		0.56
Folded-sphere container and bellows		9.22
Conical support section and inflation bottle (includes 0.50 lb of nitrogen gas for sphere inflation)		20.51
Pressure transducer and mounting bracket for X258 motor		1.23
Telemeter and umbilical sections		41.03
Interface bolts (payload to X258 motor)		0.17
Antenna and wiring harness on transition section between third and fourth stages of Scout vehicle		1.77
Container cover (foam-plastic sheet)		0.11
Thermistor (prime, spare, and potting)		0.01
Balance weights		2.49
Total payload weight for launch		96.42

inside surface. This arrangement of the laminate material simultaneously provides the requisite structural stiffness to maintain the spherical shape of the satellite without internal pressure, makes the satellite reflective of sunlight for optical tracking, provides the required electrical conductivity for a tracking beacon antenna, and helps accomplish the thermal control of the satellite. A photograph of the 12-foot-diameter inflatable sphere, fully inflated, is shown in figure 4. The sphere was fabricated from 40 flat gores of the aluminum-foil—plastic-film laminate. (See fig. 5(a) for details of a typical gore.) The gores, when bonded together, had a 0.4-inch overlapping seam. The overlapping seam did not make an electrical connection between the gores; therefore, the individual gores were electrically connected by aluminum-foil strips across the seams. Figure 5(b) is a drawing illustrating the overlapping seams and the aluminum-foil strips.

It was previously planned to rely on worldwide optical tracking of the satellite to obtain the drag data; however, in order to provide for continuous day and night tracking, a radio tracking beacon set was added to the sphere. The radio tracking beacon set required special electronic packaging techniques along with thermal control of the sphere because the lifetimes of the electronic components and storage-battery cells of the beacon set were greatly reduced for temperatures below -10° C or above 60° C. An investigation determined that proper temperature control can be obtained while the satellite is in sunlight by spotting the outside surface of the sphere with a coating having a low ratio of solar absorptance to thermal emittance and by

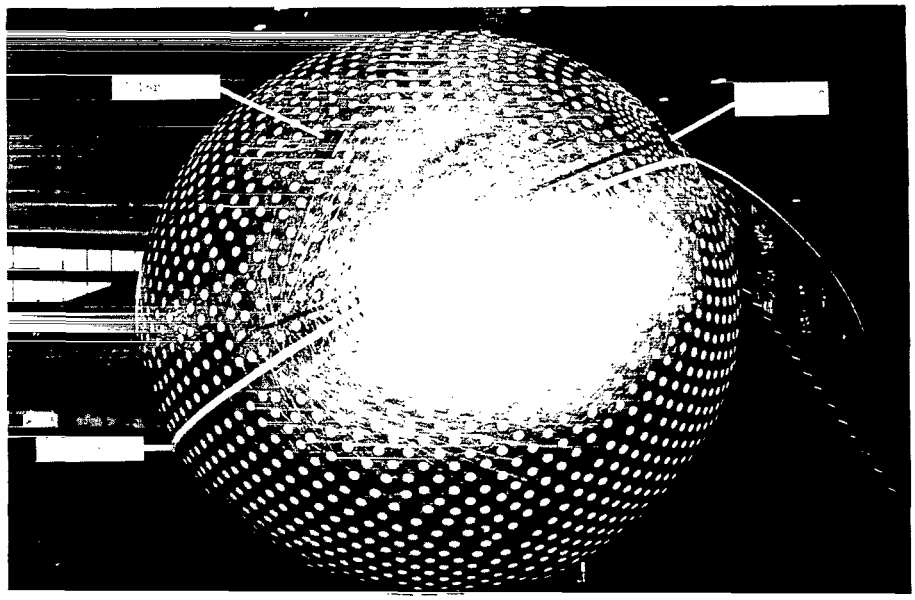

L-61-3762.1

Figure 4.- Photograph of 12-foot-diameter inflatable sphere, Explorer IX.

physically separating the beacon transmitter and battery units from the inside surface of the sphere in order to minimize the rate of heat transfer for control while the satellite is in the shadow of the earth. A detailed description of the thermal control of the Explorer IX inflatable satellite is given in reference 2.

The aluminum-foil inflatable sphere was divided into two hemispheres by a $1\frac{1}{2}$-inch-wide gap of a dielectric material, the equator, so that the two hemispheres could be used as the antenna for the tracking beacon. The fabrication details of the antenna gap are shown in figure 5(c). Ten fiber-glass stiffeners were equally spaced around the equator of the sphere and across the antenna gap because of the weakness of the dielectric material in buckling. The arrangement of the stiffeners is also shown in figure 5(c).

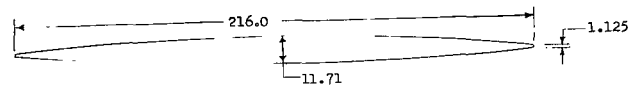

(a) Typical gore.

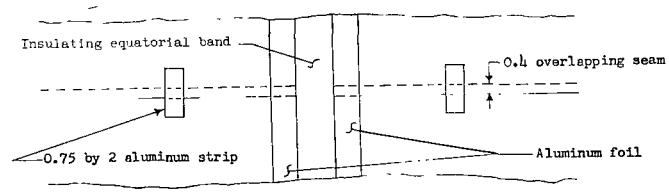

(b) Electrical continuity between gores.

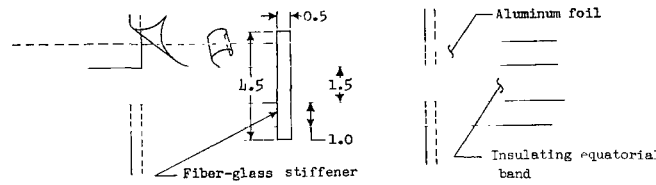

(c) General construction of antenna gap equator of plastic film.

Figure 5.- Construction and material details of 12-foot-diameter inflatable sphere. (All dimensions are in inches.)

The 12-foot-diameter inflatable sphere with the attached tracking beacon was folded into a package $8\frac{1}{2}$ inches in diameter and 11 inches long. To aid in packaging the folded sphere in the container, four pieces of foam rubber covered with aluminized plastic film were inserted into the folds of the packaged sphere. The foam-rubber pads prevented the folded sphere from packing itself tightly while vibrating during vehicle ascent.

Radio tracking beacon set for the Explorer IX satellite.- The tracking beacon set consists of seven modules: a transmitter module, a battery module, a battery switch, and four solar-cell modules. Figure 6 shows a photograph of the tracking-beacon modules. The weights of the modules are given in table I, and a description of the radio tracking beacon set is given in reference 3. The transmitter and battery modules were almost identical in weight and were located diametrically opposite on the inside surface of the sphere near the equatorial gap in order to preserve the mass balance of the inflated sphere and to facilitate the connection to the antenna. The solar-cell modules were located on the outside surface of the sphere at the apexes of an imaginary equilateral tetrahedron in order to provide continuous charging of the storage-battery cells while the satellite was in the sunlight, regardless of satellite orientation. Each of the solar-cell modules was capable of furnishing the required power and was connected in parallel to the transmitter and battery modules. All the modules were interconnected by printed cables. The size of the various modules (table III) was determined by the dimensions of the folds of the packaged sphere and the diameter of the sphere container.

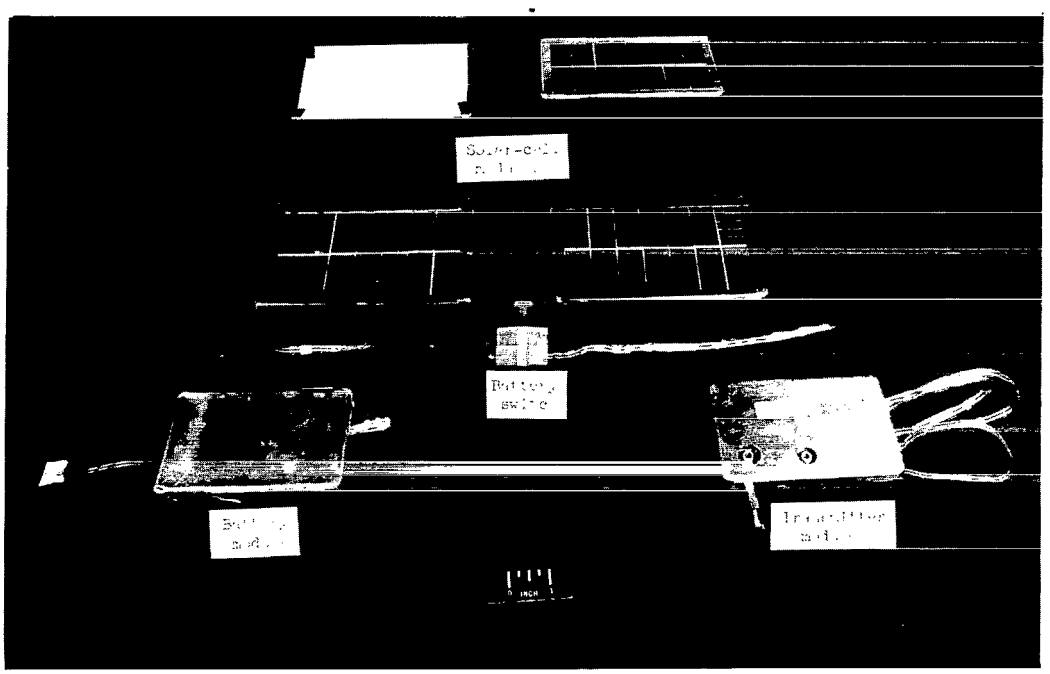

Figure 6.- Photograph of radio tracking beacon set for Explorer IX satellite. L-60-7229.1

TABLE III.- DIMENSIONS OF RADIO TRACKING BEACON MODULES

Satellite	Component	Size, in.		
		Length	Width	Height
Explorer IX	Transmitter module	4.75	3.12	0.69
	Battery module	4.75	3.12	.69
	Solar-cell module (each)	6.5	4.5	.22
	Battery switch	1.5	1.5	.12
Explorer XIX	Transmitter module	5.06	3.41	0.85
	Battery-control module	5.06	3.41	.85
	Solar-cell module (each)	6.25	4.15	.295
	Battery switch	1.5	1.5	.12

The battery switch was basically a pair of gold-plated spring-loaded contact strips separated by an insulator. As the packaged sphere unfolds after being ejected from the payload container, the insulator was pulled out to close the battery-supply circuit.

Radio tracking beacon set for the Explorer XIX satellite.- The tracking beacon set for the Explorer XIX satellite was of the same type as that for the Explorer IX satellite; however, some differences did exist. The probable cause of transmitter failure for the Explorer IX satellite was overvoltage of the transmitter. (See ref. 2.) As a result, the following modifications were made for the Explorer XIX beacon set: (1) two current regulators and six Zener diode voltage regulators were incorporated into the electronic design, and (2) a gap, vented to space, completely around the transmitter unit and a battery-control unit was utilized by suspending the units in the center of aluminum cases. Several other modifications were made to the beacon set. First, the radio-frequency (RF) power output was increased from 15 milliwatts for Explorer IX to 30 milliwatts for Explorer XIX. Second, since the Explorer XIX satellite was to be placed into a polar orbit and would pass through the radiation belts, the solar-cell shingles were mounted in aluminum containers and shielded with quartz glass covers that were 1/8 inch thick. In addition, a zinc oxide pigmented silicone elastomer was utilized as the temperature-control coating and was spotted over 25 percent of the outside surface of the Explorer XIX sphere, whereas a white epoxy enamel was spotted over 17 percent of the outside surface of Explorer IX, as was discussed in reference 2. The weights of the units and the solar-cell modules are given in table II, and their dimensions are given in table III.

Payload Subassemblies

Explorer IX subassemblies.- The subassemblies are the payload hardware necessary to transport, inflate, and separate the 12-foot-diameter sphere. The folded sphere was tranported into orbit in a cylindrical container with an inside diameter of $8\frac{1}{2}$ inches and a length of 18.7 inches. The payload container

was mated to the payload attachment collar for the Scout launching vehicle by a conical support section. (See fig. 2.) The inflation and separation system located inside the cylindrical container and conical support section consisted of an inflation bottle with a volume of 102 cubic inches containing 0.5 pound of preprocessed (dry) nitrogen gas; an ejection bellows between the inflation bottle and the folded sphere; and a disconnect mechanism connected to the inflatable sphere, the ejection bellows, and the inflation bottle. These items are shown in figure 7. The ejection bellows served two functions: first, to eject the folded sphere from the container and, second, as a plenum chamber for inflation of the sphere. A wire-rope cable of the disconnect mechanism restrains the forward movement of the sphere and the bellows after ejection of the folded sphere from the payload container. After inflation of the sphere is complete, the disconnect mechanism separates the inflated sphere from the payload container.

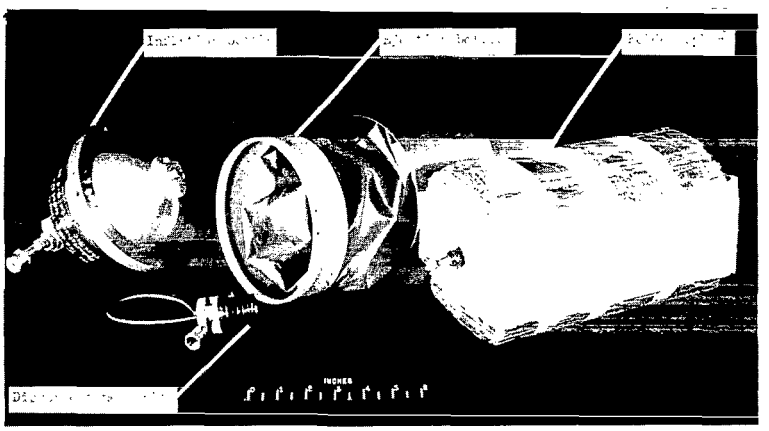

L-58-761a.1
Figure 7.- Photograph of major subassemblies of payload package of 12-foot-diameter inflatable sphere.

An activation mechanism was utilized to initiate operation of the inflation and separation system; it consisted of a pressure cell, a switch, and 6-second delay squibs initiated by rocket-chamber pressure drop at burnout of the fourth stage.

Explorer XIX subassemblies.- The subassemblies for the Explorer XIX satellite were identical to those of the Explorer IX satellite, except that the activation mechanism consisted of a timer initiated at separation of the fourth-stage rocket motor from the third stage.

ENVIRONMENTAL TESTS

Explorer IX

The complete payload was subjected to environmental tests approximately equivalent to those of one launching. The type approval tests and the flight

acceptance tests are listed in table IV. The shock tests were made by dropping the payload from a height of approximately 1 foot along the rocket-motor thrust axis. The vibration tests were performed with the use of an electrodynamic machine. The test values applied were equivalent to or greater than the vibrations and shock loads that would be experienced during the X248 (fourth-stage) firing. Figure 8(a) is a photograph of the inflating sphere 2 seconds after it is ejected from the payload container during a test of its inflation system in a vacuum chamber. The sphere is shown fully inflated in figure 8(b), just prior to separation from the payload container by the separation mechanism. Performance monitoring of the payload was carried out during the test program. The type approval and flight acceptance tests were completed without failure of the payload. Decompression, temperature, humidity, and vacuum tests were also performed, as outlined in table IV.

TABLE IV.- ENVIRONMENTAL TESTS FOR EXPLORER IX PAYLOAD

Test	Type approval			Flight acceptance		
	Acceleration amplitude, g units	Duration		Acceleration amplitude, g units	Duration	
		milliseconds	minutes		milliseconds	minutes
Shock:[a]						
Drop test[b]	30	5 to 15		30	10	
Sustained acceleration	35		3	22		3
	Frequency, cps	Amplitude, g units (rms)	Duration, minutes	Frequency, cps	Amplitude, g units (rms)	Duration, minutes
Vibration:[a]						
Sinusoidal	15 to 500	9		5 to 50	1.5	2.5
	[c]500 to 2000	[c]15	8	50 to 500	5	
				500 to 2000	10	
				525 to 625	30	.166
Gaussian random	15 to [d]2000	15		20 to [e]2000	9	2
	Remarks			Remarks		
Decompression	Payload, less fourth-stage telemeter, was subjected to altitude changes (from sea level to approximately 200,000 feet) in 8 seconds.			Payload, less fourth-stage telemeter, was subjected to altitude changes (from sea level to approximately 200,000 feet) in 40 seconds.		
Temperature	Electronic equipment, less the sphere Minitrack beacon (while nonoperative), was subjected to temperatures of -15° F for 6 hours and 140° F for 6 hours. The equipment was then stabilized at 40° F and operated.			Electronic equipment was operated for 2 hours at room conditions and self-imposed environment.		
Humidity	Electronic equipment, less the sphere Minitrack beacon (while nonoperative), was subjected to a temperature of 80° F and a relative humidity of 100 percent for 50 hours. The equipment was then operated for 1 hour after being subjected to these conditions.					
Vacuum	Payload, less fourth-stage telemeter, after completion of type approval tests, was subjected to the conditions of activation in a vacuum tank while spinning at approximately 180 rpm. The vacuum was 0.5 mm Hg.			Payload, less flight sphere, and all electronic equipment was operated by activation in a vacuum tank while spinning at approximately 180 rpm. The vacuum was 0.5 mm Hg.		

[a]Values are for an X248 rocket motor.
[b]Conducted twice for type approval test.
[c]For the frequency range from 525 to 595 cps, the amplitude rises to 25g (rms); when the frequency reaches 595 cps, the amplitude drops to 15g (rms).
[d]Decreased by 12 dB per octave, on an acceleration basis, from 1000 to 2000 cps.
[e]Decreased by 6 dB per octave, on an acceleration basis, from 1000 to 2000 cps.

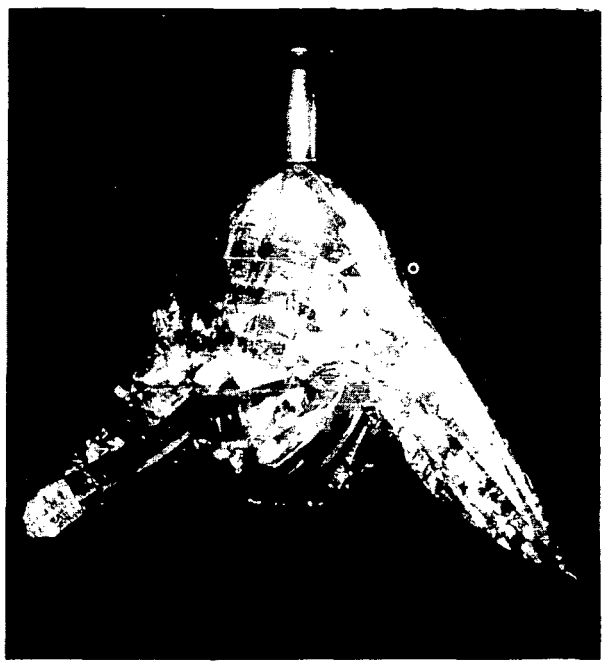

L-60-8085

(a) Time: 2 seconds after ejection from payload container.

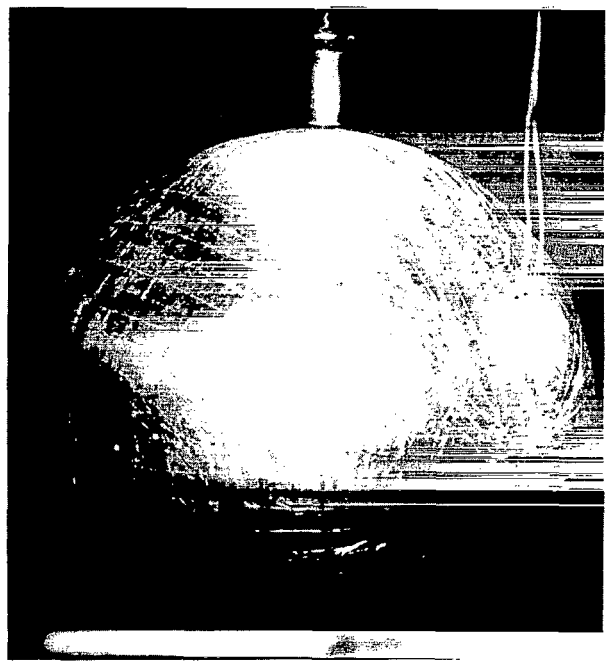

L-60-8087

(b) Sphere fully inflated; time: 150 seconds after ejection.

Figure 8.- Photographs of 12-foot-diameter sphere during inflation test in a vacuum facility.

The components of the sphere Minitrack beacon were subjected to environmental tests approximately equivalent to launching and orbiting conditions. Table V is a summary of these tests. The tests were accomplished without failure of the beacon.

TABLE V.- ENVIRONMENTAL TESTING OF COMPONENTS OF INFLATABLE-SPHERE MINITRACK BEACON

Test	Remarks
Shock	Acceleration, 50g; time, 2 to 6 milliseconds
Vibration:	
Sinusoidal	Frequency, 20 to 2000 cps; acceleration, ±3g; duration, 80 seconds Frequency, 200 to 700 cps; acceleration, ±24g; duration, 10 seconds
Gaussian random	Frequency, 200 to 700 cps; amplitude, 22.5g (rms); duration, 10 seconds
Thermal	The beacon transmitter and batteries were operated in a thermal environment between -10° C and 60° C.
Vacuum	The components of the type approval beacon after completion of the environmental tests were tested in a vacuum tank with the sphere package. The vacuum was 0.5 mm Hg.

Explorer XIX

The flight acceptance testing levels for the Explorer XIX payload are given in table VI. The tests were completed without failure of the payload. The difference in flight acceptance testing levels from those of Explorer IX is because the fourth-stage motor for the Explorer XIX launch was an X258 motor, rather than an X248 motor, as used for the Explorer IX launch.

TABLE VI.- FLIGHT ACCEPTANCE ENVIRONMENTAL TESTS FOR EXPLORER XIX PAYLOAD

Test	Remarks
Vibration:[a]	
Sinusoidal sweep frequency	Logarithmic sweep rate not greater than 4 octaves per minute. Along the thrust axis the values were as follows: Frequency range, cps: 20 to 50; 50 to 500; 500 to 2000 Acceleration amplitude, g units: ±1.0; ±4; ±8
Special sinusoidal	Logarithmic sweep rate: 1 sweep for a duration of 12 seconds at ±2g along the thrust axis only (50 to 70 cps).
Random motion	Gaussian random with normal test tolerances. Thrust: 20 to 2000 cps; 2 min; 0.03 g^2/cps; 7.7 g units (rms) Transverse: 20 to 2000 cps; 1 min; .01 g^2/cps; 4.4 g units (rms)
Spin balance[a]	The flight spacecraft was dynamically spun balanced at the nominal maximum expected flight spin rate.
Acceleration[a]	15g along thrust axis during fourth-stage burning for a period of 3 minutes. Acceleration gradient from the center of gravity not over ±10 percent. 3g along transverse axes for a period of 1 minute.
Shock[a]	Three tests to a half-sine pulse of 35g peak amplitude and for a duration from 10 to 15 milliseconds; along thrust axis only.
Vacuum	The payload, less flight sphere and all electronic equipment, was operated by activation in a vacuum tank while the payload was spinning at approximately 180 rpm. The vacuum was 0.5 mm Hg.

[a]Values are for an X258 rocket motor.

TELEMETRY

Explorer IX

The fourth stage of the Scout launching vehicle for the Explorer IX flight carried a payload telemeter in the payload compartment. The payload telemeter is included as a part of the payload package but remains with the fourth stage when the satellite is separated from the launch vehicle. The performance-events telemeter in the payload compartment was an 8-channel FM/AM type and radiated 8.5 watts of RF power at 244.3 megacycles. The payload telemeter performs as a performance telemeter during the ascent phase of the launch and as an events telemeter during the ejection, inflation, and disconnection of the satellite. For the events monitor a microswitch was used to indicate the opening of the inflation valve for the pressure bottle; two nylon and copper switches were incorporated into the disconnect mechanism to indicate, first, that the folded sphere was ejected from the payload container and, second, that the inflated sphere was separated from the container.

Explorer XIX

The fourth stage of the Scout launching vehicle for the Explorer XIX flight carried a telemeter in the payload compartment to make and relay measurements of Scout performance. However, one channel was utilized as an events monitor for the payload to indicate activation of the inflation bottle, ejection of the folded sphere from the payload container, and separation of the inflated sphere from the orbiting fourth-stage rocket motor.

RESULTS AND DISCUSSION

Explorer IX

Estimates of the lifetime of the Explorer IX satellite indicated that the lifetime of the 12-foot-diameter sphere would be greatly affected by the orbital position of perigee with respect to the sun vector and solar pressure. For a constant-energy orbit, the eccentricity would decrease if the angular momentum could be increased and would result in a decrease in apogee altitude and an increase in perigee altitude. Thus, if the orbital position of the satellite with respect to the sun could be selected to give this decrease in eccentricity, the lifetime of the satellite could be as much as 2 years (±1 year). It was recommended that the launching occur between 13:00 and 16:00 Greenwich mean time (GMT) on the February 16, 1961, launch date so that the satellite lifetime could be increased.

The Scout ST-4 (fig. 9) was launched at 13:05 GMT and the Explorer IX satellite was injected into orbit at 13:16 hours GMT on February 16, 1961, from the NASA Wallops Station. The predicted and actual orbital elements are shown in table VII. The launch time and resultant orbital parameters have resulted in a satellite lifetime of approximately 3 years.

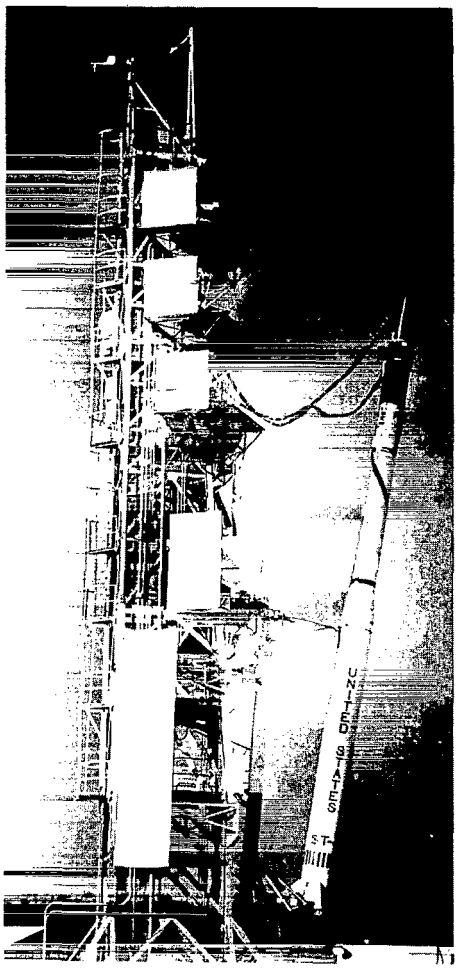

L-61-1564

Figure 9.- Photograph of Scout ST-4 vehicle for launch of Explorer IX satellite.

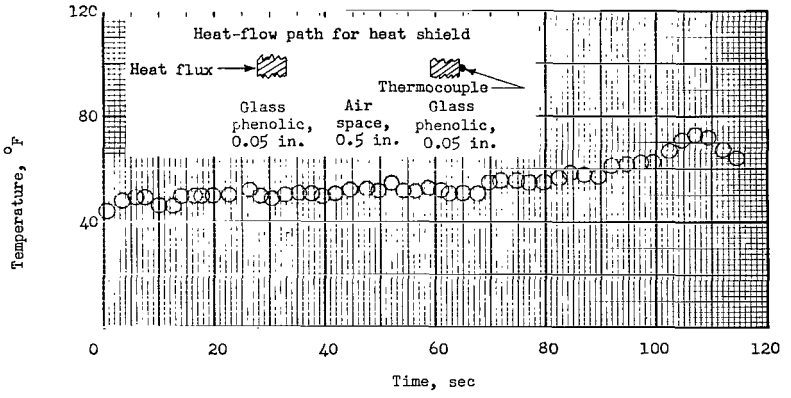

Figure 10.- Time history of temperature of inside surface of payload heat shield.

TABLE VII.- ORBITAL ELEMENTS FOR THE EXPLORER IX SATELLITE

Elements	Predicted	Actual
Perigee altitude, nautical miles	351.4	342.42
Apogee altitude, nautical miles	1434.6	1400.7
Perigee velocity, ft/sec	26,226	26,206
Apogee velocity, ft/sec	20,400	20,480
Eccentricity	0.124942	0.12263
Inclination, deg	37.93	38.91
Period, min	119.32	118.552
Injection altitude, nautical miles	351.6	363.8
Injection flight-path angle, deg	-0.06	1.80
Injection velocity, ft/sec	26,226	26,102
Injection ratio	1.06354	1.0585

Figure 10 shows the temperature on the inside surface of the payload heat shield during the first 2 minutes of ascent. The data were obtained from the telemeter installed in the transition section between the third- and fourth-stage motors of the Scout launching vehicle and indicate that the payload experienced no severe temperature environment during ascent. Figure 11 shows the sustained acceleration in the payload area during spin-up and burning of the fourth-stage rocket motor. The acceleration in the longitudinal direction was below the testing level in the flight acceptance and type approval tests. The normal and transverse accelerations resulting from the spinning fourth stage are not considered severe. Shown in figure 12 is the pressure history inside the bellows during vehicle ascent. The free-stream pressure history is also shown in the figure for vehicle ascent. Decompression tests had been made to determine whether residual air pressure in the bellows would result in premature

ejection of the payload. (See ref. 1.) The flight-test data indicate that the bellows pressure decreased during vehicle ascent as rapidly as the free-stream pressure; therefore, premature ejection of the payload was not a problem.

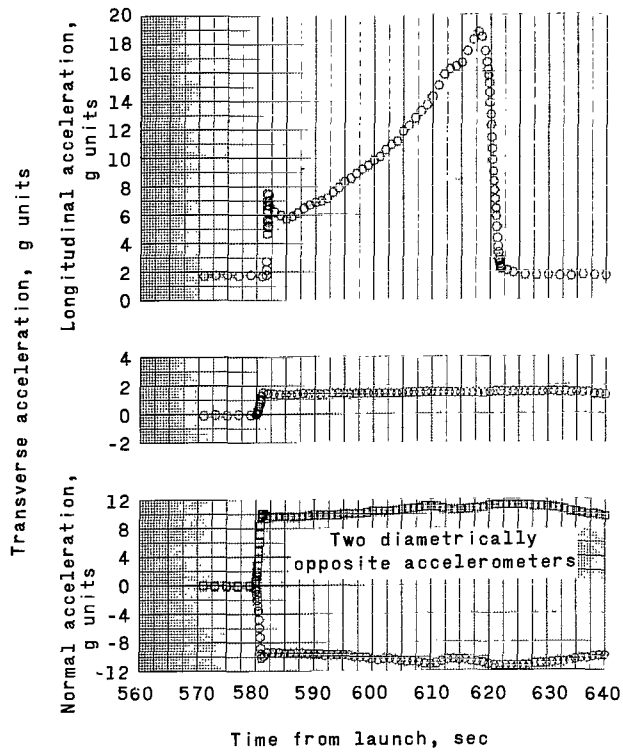

Figure 11.- Accelerations in payload area during spin-up and burning of Scout ST-4 fourth-stage rocket motor.

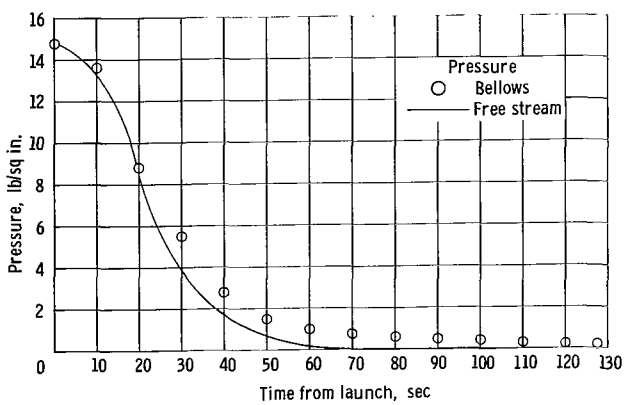

Figure 12.- Time history of payload bellows pressure during ascent of Scout ST-4 vehicle. (Note: The free-stream pressure curve is based on altitude plotted against time for Scout and U.S. Standard Atmosphere, 1962.)

The sequence of events in the ejection and inflation of the Explorer IX satellite was as follows: a pressure switch with 6-second delay squibs was activated when the chamber pressure of the fourth-stage rocket motor dropped to a predetermined value; the pressure switch fired the pyrotechnics that activated the inflation bottle; the inflation gas pressurized the bellows resulting in bellows elongation and ejection of the folded sphere; the sphere inflated to a diameter of 12 feet; finally, the inflated sphere separated from the disconnect mechanism as a spring pushed it away from the orbiting rocket motor. Shown in figure 13 is a telemeter record of the flight data for the Scout ST-4 launching of the Explorer IX satellite. The events signal indicating squib firing and activation of the inflation bottle occurred at 626.65 seconds. This time was approximately 6 seconds after the thrust-decay period of the fourth-stage rocket-motor chamber pressure, as expected. The events signal indicating ejection of the Explorer IX satellite from its payload container occurred at 627.05 seconds. The separation of the satellite from the orbiting rocket motor is shown to occur at approximately 809.2 seconds from launch. The total time of inflation was, therefore, 182.55 seconds.

Shown in figure 14 is the pressure time history inside the bellows from the time of activation of the inflation bottle to payload separation from the fourth-stage rocket motor. Figure 15 is a drawing of the ejection bellows used with the Explorer IX satellite. In figure 15(a) the bellows is shown in its folded position prior to activation of the inflation bottle. Figure 15(b) shows the

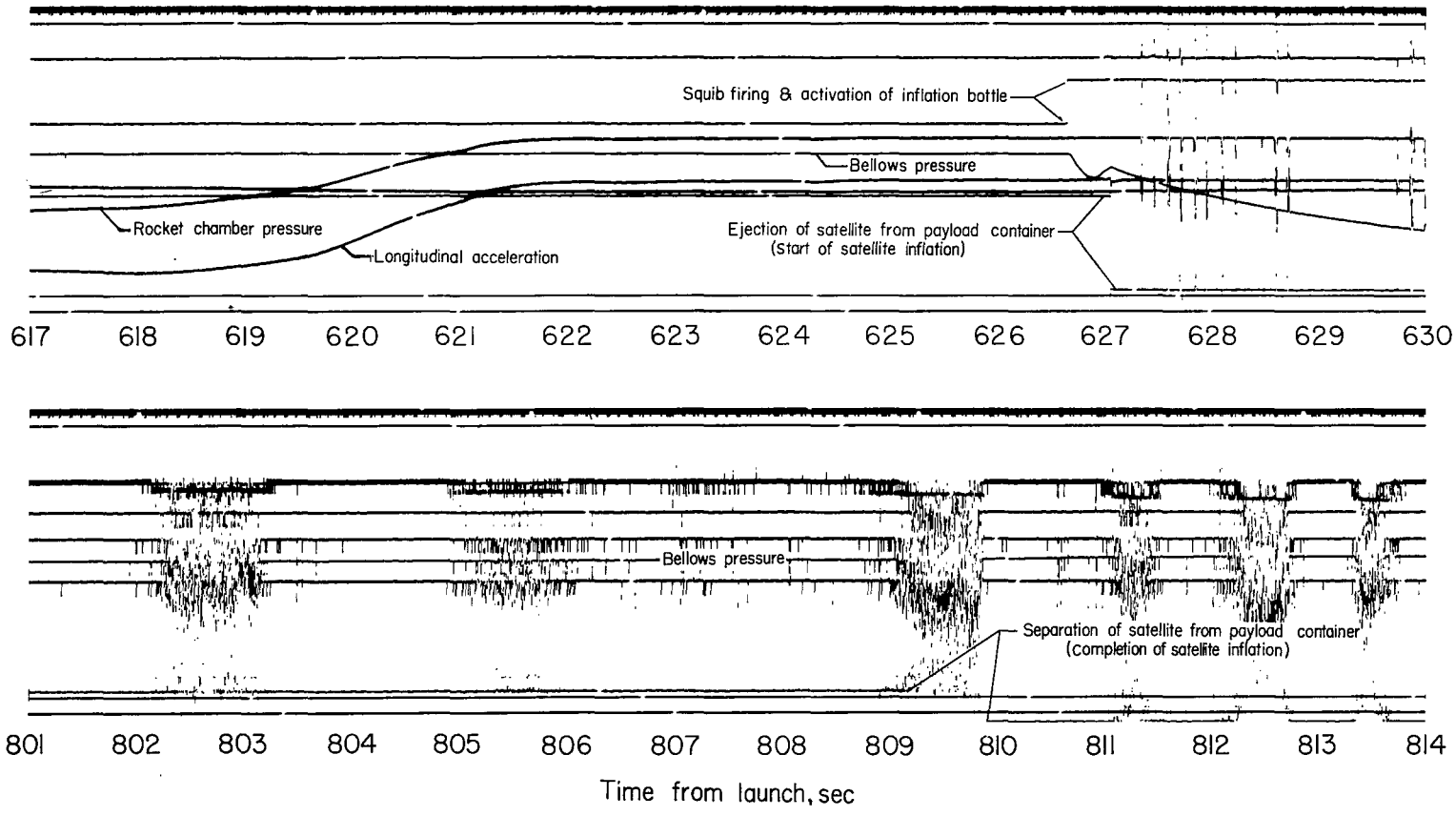

Figure 13.- Payload telemeter record of flight data for Scout ST-4 launching of Explorer IX satellite.

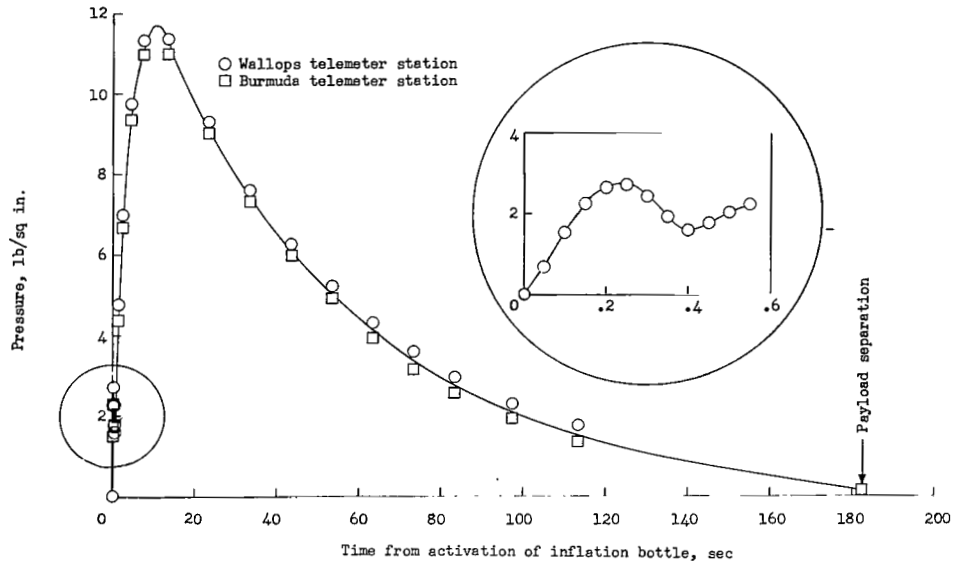

Figure 14.- Variation of payload bellows pressure with time during inflation of Explorer IX.

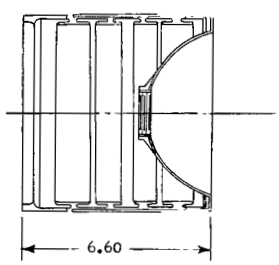

P_B = Bellows pressure

(a) Bellows in its folded position prior to activation of inflation bottle.

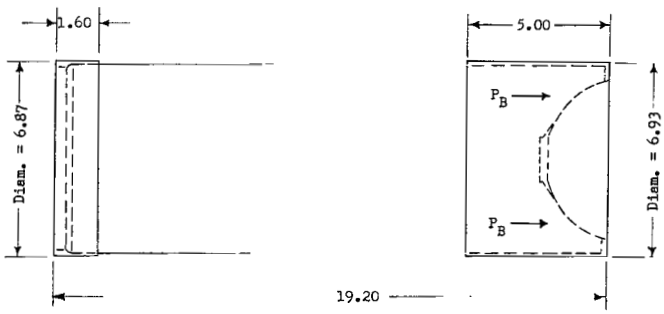

(b) Bellows at full longitudinal extension at ejection.

Figure 15.- Ejection bellows used with 12-foot-diameter inflatable sphere. (All dimensions are in inches.)

bellows at full longitudinal extension during inflation at which point the payload is ejected and is being inflated. The expansion operation of the bellows during the launch can be shown by simultaneous examination of figure 15 and the insert of figure 14. Zero time is activation of the inflation bottle. Immediately, the nitrogen inflation gas pressurizes the bellows until 0.25 second, at which time a bellows pressure decrease occurs momentarily until 0.4 second when the pressure increases again. The pressure rise between 0 and 0.25 second results from the nitrogen gas filling the bellows in its folded position. From approximately 0.20 to 0.25 second the pressure exerted on the bellows piston becomes high enough to eject the folded sphere from the payload container. Therefore, the bellows expands longitudinally until it is restrained by a wire-rope cable assembly. This bellows expansion results in a momentary pressure drop until 0.4 second, by which

time the bellows has expanded longitudinally to its maximum length and the folded sphere has been ejected. The bellows pressure again increases to 11.7 lb/sq in. during the next 10 seconds after which time the pressure begins decreasing as the nitrogen gas passes into the 12-foot-diameter sphere until the inflated sphere separates from the fourth-stage rocket motor at 182.55 seconds. (See fig. 14.)

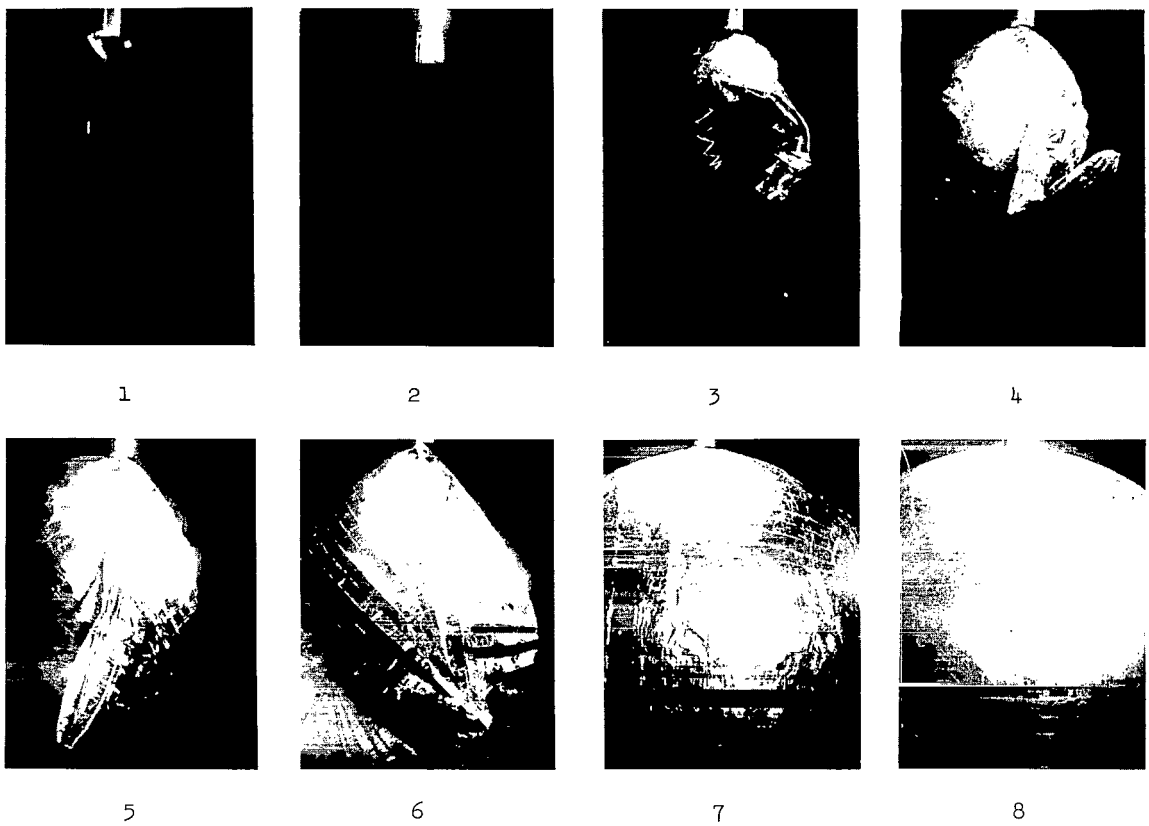

L-60-7834

Figure 16.- Photographs of a 12-foot-diameter sphere being inflated in a vacuum facility.

The mode of inflation is shown in figure 16. The figure is a photograph of a typical inflation during a development test in a vacuum facility. It can be shown that this mode of inflation was experienced in inflating the Explorer IX satellite. Prior to ignition of the fourth-stage rocket motor of the Scout launching vehicle, the rocket motor and payload were spun up to approximately 224 rpm for spin stabilization. Figure 17 is the spin-rate time history for the fourth-stage rocket motor during inflation of the Explorer IX satellite. After burnout of the rocket motor, the spin rate was 240 rpm at sphere ejection. From this time until payload separation, the only connection between the 12-foot sphere and the rocket motor is through a spherical bearing which is a part of the inflation stem. (See fig. 4(e) of ref. 1.) Steps 1 to 7 in figure 16 occur in about 18 seconds and represent the increasing of the radius of mass concentration from that of a folded condition to a sphere with a radius of almost 6 feet. This expansion of the sphere results in a large

increase in the moment of inertia of the sphere about the longitudinal or spin axis; therefore, the spin rate decreases. The orbiting configuration is then a rapidly rotating rocket motor and a slowly rotating sphere connected by a spherical bearing. The minute friction of the bearing gradually brings the spin rate of each toward an equilibrium condition or steady-state value. The reduction of the rocket-motor spin rate is shown in figure 17 between 0 and 100 seconds. However, at 100 seconds step 8 of figure 16 is approached. The pressurized sphere soon is stressed enough to make contact with the payload container, also shown in step 8 of the figure. The increase in contact between the sphere and the payload container results in a more rapid approach to an equilibrium spin rate between the two. Finally, the sphere and rocket motor are spinning at the same rate of 36.8 rpm. Based on the conservation of angular momentum, an initial spin rate of 240 rpm, and the initial configuration, the final spin rate should have been 28.4 rpm. The difference between 28.4 and 36.8 rpm is attributed to the accuracy of the measurements and to the approximations of the moment of inertia of each of the corresponding assemblies.

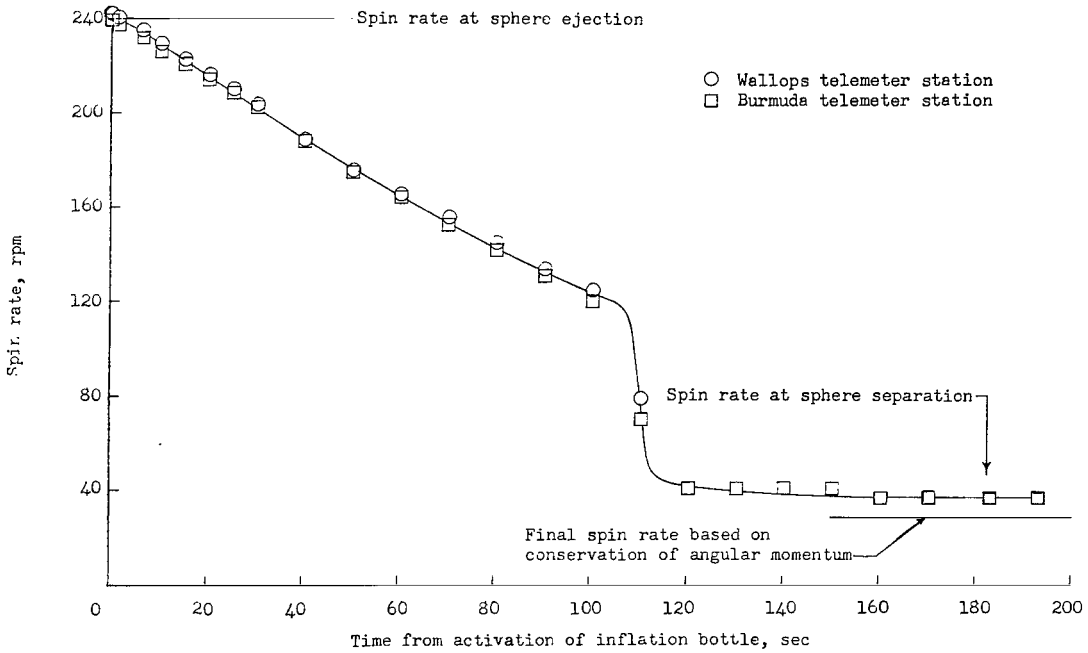

Figure 17.- Variation of spin rate with time for Scout ST-4 fourth-stage rocket motor during inflation of Explorer IX satellite.

As was previously mentioned, the ejection, inflation, and separation of the sphere was accomplished in 182.55 seconds. This timing was nearly 90 seconds sooner than the time indicated in the series of development tests performed in a vacuum facility. Figure 18 is a drawing of the disconnect mechanism between the sphere and the payload container. On the left-hand side of the figure the disconnect mechanism is shown in its position relative to the earth during the development tests; on the right-hand side of the figure the mechanism is shown in its position relative to the earth during separation in orbit. For payload separation to occur, the valve spring must push the bellows piston assembly toward the wire-rope cable assembly. During a development

test, the spring force must overcome the pressure force of the bellows and also lift the weight of the bellows piston for separation to occur. In orbit the spring force has only to overcome the pressure force of the bellows; therefore, for a given spring force a larger pressure force can be overcome in orbit than in a development test. Since the bellows pressure is decreasing with time prior to separation, the separation would occur earlier in orbit than in a development test with the payload in a vertical condition.

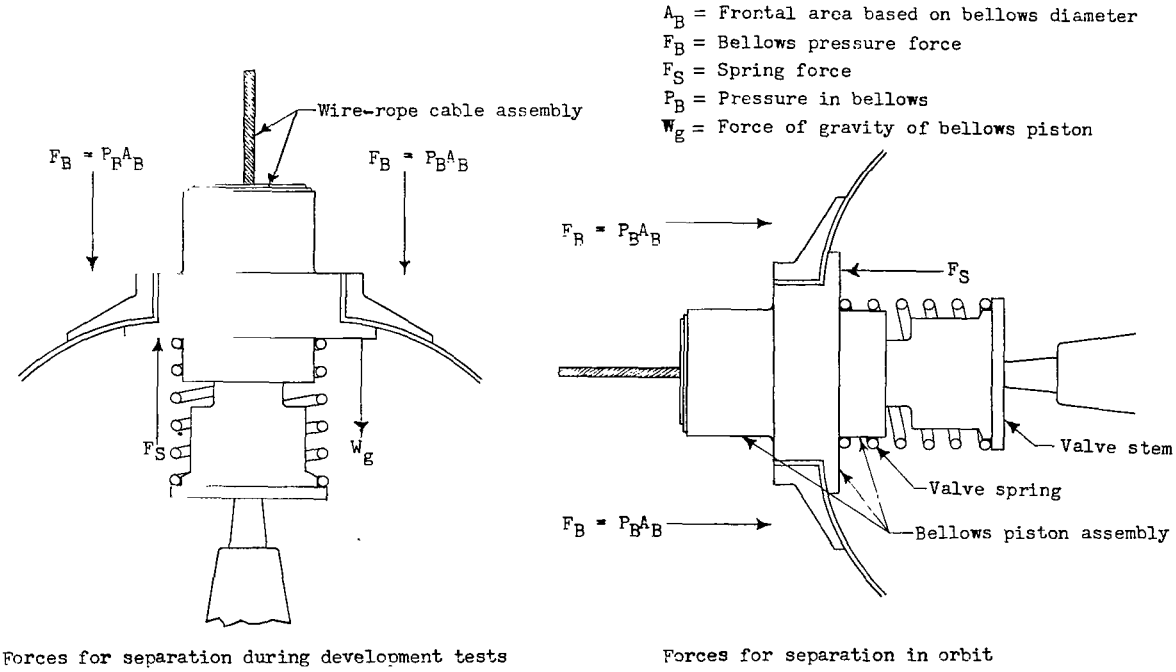

Figure 18.- Orientation of disconnect mechanism between sphere and payload container during separation for a development test and during separation in orbit.

Having completed the necessary steps for ejection, inflation, and separation in orbit, the Explorer IX satellite would appear as shown in the cutaway drawing in figure 19. Because optical tracking of the Explorer IX satellite was to be the primary method of satellite acquisition, the degree of optical visibility of the inflated 12-foot-diameter sphere illuminated by the sun while in a satellite orbit had to be determined. In order to predict the optical visibility of the inflated sphere, it was first necessary to determine whether the satellite reflected as a diffuse or specular sphere and what its albedo would be. It was determined in reference 1 that the aluminum sphere was essentially a specular reflector with an albedo of 79 percent. Reference 4 indicated that the white epoxy paint which was spotted over the outside surface of the sphere was approximately a diffuse reflector. Figure 20 presents the apparent magnitude at zenith of a specular 79-percent-reflectivity 12-foot-diameter spherical satellite plotted against distance of satellite from the observer. Also shown in figure 20 is the apparent magnitude of the sphere with 83 percent of the area reflecting as a specular reflector and 17 percent of the area reflecting as a diffuse reflector. The values of 83 percent and 17 percent

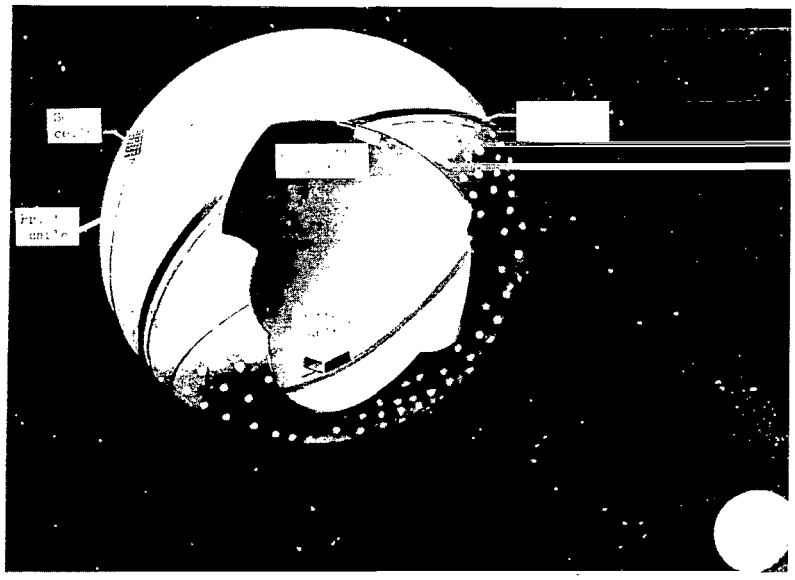

L-60-7809.2

Figure 19.- Cutaway drawing of the Explorer IX satellite in orbit.

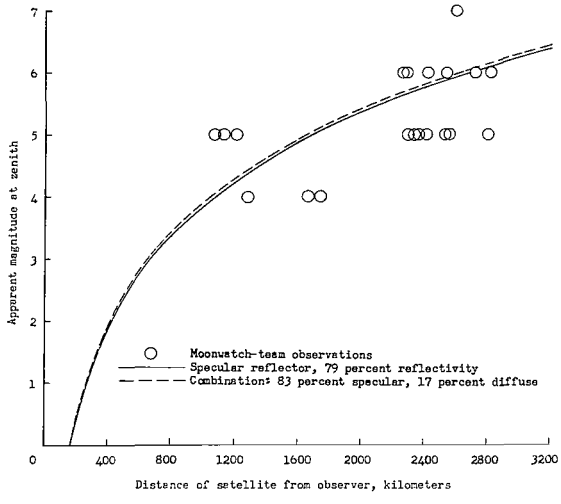

Figure 20.- Apparent magnitude at zenith for Explorer IX satellite for a nighttime sky.

represent, respectively, the percentage surface area of aluminum and of white epoxy paint for the Explorer IX satellite. A discussion of the calculations necessary for determining the apparent magnitude is given in the appendix. During its lifetime in orbit, the Explorer IX sphere is observed by various Moonwatch teams located throughout the world. The Moonwatch teams record the apparent magnitude of orbiting objects. Their observations for the Explorer IX satellite are shown in figure 20 for comparison with the theoretical curves. The data are considered to be in excellent agreement with the theoretical curves because of the many variations that can affect the observations. The observed magnitudes are estimated to the nearest whole number by comparison with a star, and no correction is made for atmospheric attenuation.

Explorer XIX

The Scout 122 vehicle was launched at 18:49 GMT, and the Explorer XIX satellite was injected into orbit at 18:59 GMT on December 19, 1963, from the Pacific Missile Range. The events monitoring channel indicated that the 12-foot sphere was ejected and separated. Radar cross-section observations indicated that the sphere was fully inflated. The Moonwatch teams made observations of the Explorer XIX sphere and reported that it was not scintillating in brightness and was of the appropriate magnitude expected. Thus it was concluded that the Explorer XIX sphere was fully inflated. The successful ejection and inflation of the Explorer XIX satellite again demonstrated that the folded sphere will not eject prematurely. The radio tracking beacon continues to operate, except that the signal level is from -135 to -140 dBm and acquisition is extremely difficult. The predicted and actual orbital elements are shown in table VIII.

TABLE VIII.- ORBITAL ELEMENTS FOR THE EXPLORER XIX SATELLITE

Elements	Predicted	Actual
Perigee altitude, nautical miles	322.1	319.6
Apogee altitude, nautical miles	1616.0	1290.8
Semi-major axis, nautical miles	4412.46	4249.26
Eccentricity	0.14667	0.11429
Inclination, deg	78.497	78.618
Argument of perigee, deg	165.381	160.815
Period, min	122.557	115.791
Injection altitude, nautical miles	322.1	323
Injection flight-path angle, deg	0	0.6
Injection velocity, ft/sec	26,562	26,162

CONCLUDING REMARKS

A study has been made of the flight-test results for the launch and orbiting of the 12-foot-diameter inflatable spheres, Explorer IX and Explorer XIX. The two flight tests have demonstrated that, in general, the in-flight operation of the ejection and inflation system performed as was expected from environmental tests. The inflation of both spheres has indicated that a structure that is lightweight and delicate can be ejected, inflated, and separated from a launching vehicle after being exposed to the environment imposed by an orbital launch which includes speeds of 26,000 feet per second and for the Scout vehicle spin rates between 160 and 240 rpm.

The two flight tests have demonstrated that the longitudinally unrestrained folded sphere will not eject prematurely. The flight-test results for the launch of Explorer IX indicated that separation of the inflated sphere while in orbit can be expected to occur in less time than during environmental tests performed in a vertical configuration.

Optical observations of the orbiting sphere agree very well in apparent magnitude with the design calculations for the apparent magnitude of this type of satellite. The events monitoring channel of the payload telemeter indicated that the Explorer XIX satellite was ejected and separated. Optical and radar observations of the Explorer XIX satellite have indicated that it also is fully inflated.

Langley Research Center,
National Aeronautics and Space Administration,
Langley Station, Hampton, Va., June 4, 1964.

APPENDIX

OPTICAL VISIBILITY OF A SPHERICAL SATELLITE

SYMBOLS

a	albedo or reflectance
E	illumination at observer on earth, foot-candles
H	elevation angle of sun above horizon
h	distance from satellite to observer, ft
I	luminous intensity of satellite in direction of observer, (foot-candles)(sq ft)
m	stellar magnitude
r	radius of spherical satellite, ft
α	elevation angle above horizon
θ	phase angle, radians

DEVELOPMENT OF EQUATIONS

In reference 5, the basic equations were derived for determining the observed illumination from a sphere reflecting sunlight at a distance from the observer for both a diffused and a purely specular sphere. In reference 6 a detailed method is formulated for calculating the illumination at the observer on earth from a purely diffused sphere. In both reports the illumination at the observer was increased by the square of the radius of the sphere and decreased by the square of the distance from the sphere to the observer. The equation for the illumination at the observer on earth is

$$E = \frac{I}{h^2} e^{-0.117 \csc \alpha} \tag{1}$$

The value of the attenuation coefficient, 0.117, occurs when there is a very clear sky, an elevation of 10,000 feet, and approximately 3 mm of ozone (ref. 6). The value of the luminous intensity per unit area of the sphere in the direction of the observer depends upon whether the sphere has a diffused or specular reflecting surface.

If the sphere has a perfectly diffusing surface obeying Lambert's law, the light reflected by the sphere should vary with the phase angle, as shown in reference 7, where the phase angle is defined as the angle between the direction to the sun and the line of sight to the observer. The expression for the phase angle θ is $\alpha + H$. Reference 8 gives the illumination due to the sun and outside of the earth's atmosphere as 12,700 foot-candles. The luminous intensity of the satellite of radius r in the direction of the observer (ref. 7) is, therefore,

$$I_{\text{diffuse sphere}} = a \frac{2}{3} \frac{12,700}{\pi} \left[\frac{\sin \theta + (\pi - \theta)\cos \theta}{\pi} \right] \pi r^2 \qquad (2$$

Combining equations (1) and (2) gives the following relation for the illumination observed on the surface of the earth for a diffusely reflecting sphere illuminated by the sun

$$E_{\text{diffuse sphere}} = a \frac{2}{3} 12,700 \left[\frac{\sin \theta + (\pi - \theta)\cos \theta}{\pi} \right] \frac{r^2}{h^2} e^{-0.117 \csc \alpha} \qquad (3$$

For a purely specular sphere, the luminous intensity I is independent o the phase angle while being one-fourth of the incident flux or illumination (ref. 5). The equation for this relationship is

$$I_{\text{specular sphere}} = \frac{12,700}{4\pi} a \pi r^2 \qquad (4$$

For a specular reflecting sphere, the illumination observed on the surface of the earth is obtained by combining equations (1) and (4). This illumination is

$$E_{\text{specular sphere}} = a \frac{12,700}{4} \frac{r^2}{h^2} e^{-0.117 \csc \alpha} \qquad (5)$$

Once the illumination at the observer on earth is known, the stellar magnitude m of the sphere, when seen at any distance by an observer, can be calculated by the following equation:

$$m = -2.5 \log E - 16.46 \qquad (6)$$

REFERENCES

1. Coffee, Claude W., Jr., Bressette, Walter E., and Keating, Gerald M.: Design of the NASA Lightweight Inflatable Satellites for the Determination of Atmospheric Density at Extreme Altitudes. NASA TN D-1243, 1962.

2. Woerner, Charles V., and Keating, Gerald M.: Temperature Control of the Explorer IX Satellite. NASA TN D-1369, 1962.

3. Anon.: Radio Beacon Set for 12-Foot Inflatable Satellite. AED 404 (Contract No. NAS 1-863), Radio Corp. of America, Mar. 1961.

4. Keating, Gerald M., and Mullins, James A.: Vectorial Reflectance of the Explorer IX Satellite Material. NASA TN D-2388, 1964.

5. Zirker, J. B., Whipple, F. L, and Davis, R. J.: Time Available for the Optical Observation of an Earth Satellite. Scientific Uses of Earth Satellites, James A. Van Allen, ed., Univ. of Michigan Press (Ann Arbor), c.1956, pp. 23-28.

6. Tousey, R.: The Visibility of an Earth Satellite. Astronautica Acta, Vol. II, Fasc. 2, 1956, pp. 101-112.

7. Russell, Henry Norris: On the Albedo of the Planets and Their Satellites. The Astrophysical Jour., vol. XLIII, no. 3, Apr. 1916, pp. 173-196.

8. Johnson, Francis S.: The Solar Constant. Jour. Meteorology, vol. 11, no. 6, Dec. 1954, pp. 431-439.

2.17125
46

"The aeronautical and space activities of the United States shall be conducted so as to contribute . . . to the expansion of human knowledge of phenomena in the atmosphere and space. The Administration shall provide for the widest practicable and appropriate dissemination of information concerning its activities and the results thereof."

—NATIONAL AERONAUTICS AND SPACE ACT OF 1958

NASA SCIENTIFIC AND TECHNICAL PUBLICATIONS

TECHNICAL REPORTS: Scientific and technical information considered important, complete, and a lasting contribution to existing knowledge.

TECHNICAL NOTES: Information less broad in scope but nevertheless of importance as a contribution to existing knowledge.

TECHNICAL MEMORANDUMS: Information receiving limited distribution because of preliminary data, security classification, or other reasons.

CONTRACTOR REPORTS: Technical information generated in connection with a NASA contract or grant and released under NASA auspices.

TECHNICAL TRANSLATIONS: Information published in a foreign language considered to merit NASA distribution in English.

TECHNICAL REPRINTS: Information derived from NASA activities and initially published in the form of journal articles.

SPECIAL PUBLICATIONS: Information derived from or of value to NASA activities but not necessarily reporting the results of individual NASA-programmed scientific efforts. Publications include conference proceedings, monographs, data compilations, handbooks, sourcebooks, and special bibliographies.

Details on the availability of these publications may be obtained from:

SCIENTIFIC AND TECHNICAL INFORMATION DIVISION

NATIONAL AERONAUTICS AND SPACE ADMINISTRATION

Washington, D.C. 20546